Stationary and dynamical descriptions of strong correlated systems

E. C. Goldberg,[1] F. Flores,[2] and R. C. Monreal[2]

[1]*Instituto de Desarrollo Tecnológico (CONICET-UNL) and Facultad de Ingeniería Química, UNL, cc91, 3000 Santa Fe, Argentina*
[2]*Departamento de Física Teórica de la Materia Condensada, C-V, Universidad Autónoma de Madrid, E-28049 Madrid, Spain*

This work is mainly devoted to the description of processes that involve the interaction between an atom and a surface, in which a strong Coulomb repulsion on the atomic site (U) limits the charge exchange to one electron (infinite-U limit). In this limit, the Anderson Hamiltonian for a many-fold (N) of states localized on the atomic site can be represented in terms of auxiliary bosons and physical operators in the mixed boson-electron space can be defined. In this work the Hamiltonian is solved by defining appropriate Green's functions for physical operators. Then we solved the equations of motion of these Green's functions, up to a second order in the atom-surface coupling, either for the stationary case or for a real time-dependent problem. We show that our approach reproduces the known exact results in the nondegenerate ($N=1$) case, and for $N>1$ gives excellent agreement with exact calculations and approximations valid for large N (the $1/N$ expansion). Finally, the accurate description of dynamical processes is shown by the comparison with the exact results available for a small four-level system. In this case we also compare with results obtained by using the noncrossing approximation and with the usual spinless model calculation.

PACS number(s): 79.20.Rf, 34.50.Fa

I. INTRODUCTION

An accurate description of the interaction between atomic localized states and the conduction electrons of a metal is a matter of constant interest due to the importance this subject has in many different physical problems as magnetic impurities in metals,[1,2] quantum dots coupled to electronic reservoirs,[3] and atoms moving outside a metal surface.[4–8] The two-electron terms related with either intrasite or intersite Coulomb repulsions represent the main complexity for solving this kind of problems. Different approximations are attempted depending on the particular features of the interacting system. A mean-field approximation is adequate, in general, for small values of the Coulomb terms, and a perturbative correction up to a higher order when they are not small enough compared with the one-electron interactions involved. In the opposite limit, that is a strong electronic repulsion, the zeroth order includes the electron-electron repulsion and the one-electron interactions are the perturbative terms. The Anderson model first introduced to describe a magnetic impurity in a metal,[9] has played a very important role in the later developments related with the interaction between extended and localized states. This model can be extended in a straightforward way to nonequilibrium problems as is the case of ion-surface collisions and allows us to include different kind of interactions between the localized electrons (direct and exchange Coulomb terms).

This work is mainly devoted to the description of processes that involve the interaction between an atom and a surface, in which a strong electronic correlation (U) on the atom site limits the charge exchange to one electron (infinite-U limit). The slave-boson approach to the Anderson Hamiltonian provides a fair description of a many-fold (N) of strongly correlated states localized on the atom site.[10] In this work we will solve this Hamiltonian using the equation of motion (EOM) method for the time-dependent Green functions introduced by Keldysh[11] and defined in the boson-electron mixed space. We will show that a solution of the equations of motion up to a strict second order in the atom-surface coupling gives a very good approximate method to solve either the stationary or the dynamical interaction process. The EOM has been previously used in the stationary case and in the limit of large values of U, by considering a pure fermion description and only the spin momentum projection ($N=2$),[12–15] but a consistent second-order solution has not been found in these works. Other very used method is the one based on the noncrossing approximation (NCA),[10,16] that has been also generalized to the time-dependent nonequilibrium situation a while ago.[4–7] The formalism developed in this work accounts for the same rate equations obtained by the NCA, and also for the exact time evolution in the $N=1$ case. The augmented power of the EOM method when applied to time-dependent processes can be shown through the comparison with the exact results available in the case of a four-level system.[17] This discrete model system has been used in a previous work to study a perturbative calculation up to a second order of the on-site electronic correlation term within a dynamical evolution.[18] In that case it was found an excellent agreement with the exact results within a range of values of the correlation term comparable to those of the one-electron hopping, for which the second order treatment cannot be justified in the stationary case. A similar analysis is performed in this work by comparing our approach to the infinite-U limit with the exact results. The usual approximation for strong intra-atomic Coulomb repulsion based on the use of only one active state localized on the atom site (the spinless model) and the NCA results for this four-level system are also analyzed.

II. MODEL AND THEORETICAL ANALYSIS

A. Model

In this work we consider the case of an atomic level ε_m interacting with a metal surface defined by the k states of

energies ϵ_k. We are interested in the case of a high intra-atomic Coulomb interaction U, which can be described by means of the following slave-boson Hamiltonian:[10]

$$H(t) = \sum_{km} \epsilon_k n_{km} + \sum_m \varepsilon_m d_m^+ d_m + \sum_{km} [V_k c_{km}^+ (b^+ d_m) + V_k^* (d_m^+ b) c_{km}], \tag{1}$$

where an auxiliary boson field, b and b^+, is introduced; and it is considered a N-fold fermion state with m denoting the angular momentum projection ($j, m_j = m$). The constraint relation

$$b^+ b + \sum_m d_m^+ d_m = Q = 1 \tag{2}$$

is imposed to guarantee that no more than 1 electron occupies the atomic d level.

We are going to analyze the time-dependent solution of Eq. (1) using the Green function technique. The Keldysh-Green functions[11] appropriate for the physical operators $b^+(t)d_m(t)$ and $d_m^+(t)b(t)$ of this problem are

$$G_{mm}(t,t') = i\langle \Phi_0 | \{d_m^+(t')b(t'), b^+(t)d_m(t)\} | \Phi_0 \rangle \Theta(t'-t), \tag{3}$$

$$F_{mm}(t,t') = i\langle \Phi_0 | [d_m^+(t')b(t'), b^+(t)d_m(t)] | \Phi_0 \rangle. \tag{4}$$

{ } and [ ] being the anticonmutator and the conmutator of the corresponding operators respectively; and the initial state $|\Phi_0\rangle = |0; Q=1\rangle$ is the direct product of the unperturbed Fermi sea by the state with one boson and none fermion (or none hole) in the localized d state. It is important to notice that

$$G_{mm}(t \rightarrow t', t') = i\langle n_m + n_b \rangle, \tag{5}$$

$$F_{mm}(t = t', t') = i\langle n_m - n_b + 2n_m n_b \rangle = i\langle n_m - n_b \rangle, \tag{6}$$

where we have used that $\langle n_m n_b \rangle = 0$ according with the infinite-U limit and $\langle n_b \rangle = 1 - \sum_{m'} \langle n_{m'} \rangle$.

B. The equations of motion for the $G_{mm}(t,t')$

By using Eq. (1) we obtain the following equation of motion for the advanced Green function $G_{mm}(t,t')$:

$$idG_{mm}(t,t')/dt = z_m \delta(t-t') + \varepsilon_m G_{mm}(t,t') + \sum_k V_k(t) G_m(c_{km})$$
$$+ \sum_{k, m' \neq m} V_k(t) G_m(d_{m'}^+ d_m c_{km'})$$
$$- \sum_{k, m' \neq m} V_k(t) G_m(n_{m'} c_{km}), \tag{7}$$

where $z_m = \langle n_m + n_b \rangle$, and the following notation is used:

$$G_m(A) = i\langle \Phi_0 | \{d_m^+(t')b(t'), A(t)\} | \Phi_0 \rangle \Theta(t'-t).$$

where $A = c_{km}, d_{m'}^+ d_m c_{km'}, n_{m'} c_{km}$ in the different terms of Eq. (7). The equations of motion of these new Green functions are.

$$idG_m(c_{km})/dt = \epsilon_k G_m(c_{km}) + V_k G_{mm}, \tag{8}$$

$$idG_m(d_{m'}^+ d_m c_{km'})/dt$$
$$= -\langle d_{m'}^+ b c_{km'} \rangle_{t'} \delta(t-t') + (\varepsilon_m - \varepsilon_{m'} + \epsilon_k) G_m(d_{m'}^+ d_m c_{km'})$$
$$- V_k(t) G_m(n_{m'} d_m b^+) + \sum_K V_K(t) G_m(c_{Km'}^+ c_{km'} b^+ d_m)$$
$$- \sum_K V_K(t) G_m(d_{m'}^+ c_{km'} b c_{Km}), \tag{9}$$

$$idG_m(n_{m'} c_{km})/dt = \epsilon_k G_m(n_{m'} c_{km}) + V_k(t) G_m(n_{m'} d_m b^+)$$
$$+ \sum_K V_K(t) [G_m(d_{m'}^+ b c_{Km'} c_{km})$$
$$- G_m(c_{Km'}^+ d_{m'} b^+ c_{km})]. \tag{10}$$

The $G_m(n_{m'} d_m b^+)$ is zero identically because it is not possible to have at the same time one electron in m and another in $m' \neq m$. Here we have to remark the differences with a previous work[19] where an incorrect $\langle n_{m'} \rangle G_{mm}$ approximation to this function is assumed and the equal time value of the $G_m(d_{m'}^+ d_m c_{km'})$ function is neglected. Instead of calculating the new Green functions that appear in Eqs. (9) and (10), one can follow the approach proposed by Lacroix[14] for the static case and make the following mean-field-like decouplings:

$$G_m(c_{Km'}^+ c_{km'} b^+ d_m) = \langle c_{Km'}^+ c_{km'} \rangle_t G_{mm}(t,t'), \tag{11}$$

$$G_m(d_{m'}^+ c_{km'} b c_{Km}) = \langle d_{m'}^+ b c_{km'} \rangle_t G_m(c_{Km}). \tag{12}$$

However, one of the goals of this work is to show that a strict solution to order V^2 of Eqs. (9) and (10) provides a fair better solution. This implies the following approximations:

$$G_m(c_{Km'}^+ c_{km'} b^+ d_m) = \langle n_{km'} \rangle_0 G_{mm}(t,t') \delta_{Kk} + O(V^2), \tag{13}$$

$$G_m(d_{m'}^+ c_{km'} b c_{Km}) = O(V^2), \tag{14}$$

where $\langle n_{km} \rangle_0$ is the km-state occupation for $V_k = 0$, that in the case of a metal surface is given by the Fermi distribution (E_F denotes the Fermi energy, k_B the Boltzman constant and T the absolute temperature):

$$\langle n_{km} \rangle_0 = n_{km} = \frac{1}{1 + \exp[(\epsilon_{km} - E_F)/k_B T]}.$$

In the following and for the sake of simplicity, we write down the equations of motion for the Green's functions to order V^2, but another set of equations of motion can be easily

derived with the mean-field decoupling of Eqs. (11) and (12) in an analogous way. Results with both kind of approximations will be presented in the next section, however. After some algebra, the final equation for $dG_{mm}(t,t')/dt$ is

$$
idG_{mm}(t,t')/dt = z_m \delta(t - t') + \varepsilon_m G_{mm}(t,t')
$$
$$
- i \sum_{k, m' \neq m} V_k(t) \langle d^+_{m'} b c_{km'} \rangle_{t'} e^{-i(\varepsilon_m - \varepsilon_{m'} + \epsilon_k)(t - t')}
$$
$$
+ \int_t^{t'} d\tau [\Xi^A(t, \tau) + \Xi^{A<}_m(t, \tau)] G_{mm}(\tau, t'),
$$

(15)

where

$$
\Xi^A(t, \tau) = i\Theta(\tau - t) \sum_k V_k(t) V_k(\tau) e^{i\epsilon_k(\tau - t)},
$$

(16)

$$
\Xi^{A<}_m(t, \tau) = \Xi^{A<}_m(t, \tau)
$$
$$
= i\Theta(\tau - t) \sum_{k, m' \neq m} V_k(t) V_k(\tau) n_{km'} e^{-i(\varepsilon_m - \varepsilon_{m'} + \epsilon_k)(t - \tau)}.
$$

(17)

C. The equations of motion for the $F_{mm}(t,t')$

In the case of $F_{mm}(t,t')$, the equation of motion is

$$
idF_{mm}(t,t')/dt = \varepsilon_m F_{mm}(t,t') + \sum_k V_k(t) F_m(c_{km})
$$
$$
+ \sum_{k, m' \neq m} V_k(t) F_m(d^+_{m'} d_m c_{km'})
$$
$$
- \sum_{k, m' \neq m} V_k(t) F_m(n_{m'} c_{km}).
$$

The following notation is now introduced:

$$
F_m(A) = i \langle \Phi_0 | [d^+_m(t') b(t'), A(t)] | \Phi_0 \rangle.
$$

The equations of motion for the $F_m(A)$ are calculated by a complete similar procedure to that for the G functions. The main differences arise from the boundary conditions at the initial time t_0. It can be shown that the following relations are satisfied:

$$
F_m[c_{km}(t_0)] = [2n_{km} - 1] G_m[c_{km}(t_0)],
$$

$$
F_m[d^+_{m'} d_m c_{km'}(t_0)] = [2n_{km'} - 1] G_m[d^+_{m'} d_m c_{km'}(t_0)],
$$

$$
F_m[n_{m'} c_{km}(t_0)] = [2n_{km} - 1] G_m[n_{m'} c_{km}(t_0)].
$$

These kind of relations make necessary to know the G_{mm} functions for calculating the F_{mm} ones. Finally, the V^2 order solution to the equation of motion results

$$
idF_{mm}(t,t')/dt = \varepsilon_m F_{mm}(t,t') - i \sum_{k, m' \neq m} (2n_{km'} - 1) V_k(t)
$$
$$
\times \langle d^+_{m'} b c_{km'} \rangle_{t'} e^{-i(\varepsilon_m - \varepsilon_{m'} + \epsilon_k)(t - t')}
$$
$$
+ \int_{t_0}^t d\tau [\Xi^R(t, \tau) + \Xi^{R<}_m(t, \tau)] F_{mm}(\tau, t')
$$
$$
+ \int_{t_0}^{t'} d\tau [\Omega(t, \tau) + \Omega^<_m(t, \tau)] G_{mm}(\tau, t'),
$$

(18)

where it has been defined as

$$
\Omega(t, \tau) = i \sum_k (2n_{km} - 1) V_k(t) V_k(\tau) e^{i\epsilon_k(\tau - t)},
$$

(19)

$$
\Omega^<_m(t, \tau) = i \sum_{k, m' \neq m} (2n_{km'} - 1) V_k(t) V_k(\tau) n_{km'} e^{-i(\varepsilon_m - \varepsilon_{m'} + \epsilon_k)(t - \tau)}
$$

(20)

and the retarded self-energies Ξ^R are related to the advanced ones Ξ^A by the equations

$$
\Xi^R(t, \tau) = [\Xi^A(\tau, t)] * ,
$$

$$
\Xi^{R<}_m(t, \tau) = [\Xi^{A<}_m(\tau, t)] * .
$$

D. Analysis of the numerical solution to the integrodifferential equations

For time-dependent processes where the initial time value t_0 corresponds to the noninteracting situation ($V_k = 0$), the following quantities are well defined:

$$
\langle n_m(t_0) \rangle = 0,
$$

$$
\langle d^+_m b c_{km} \rangle_{t_0} = 0,
$$

$$
\langle c^+_{Km} c_{km} \rangle_{t_0} = n_{km} \delta_{Kk}.
$$

To solve the integrodifferential equations (15) and (18) for the $G_{mm}(t,t')$ and $F_{mm}(t,t')$ respectively, implies to evolve along the two time values: t' that varies from t_0 to $t_{max}(\rightarrow \infty)$, and t from t_0 to t', for each t' value. But $G_{mm}(t,t')$ and $F_{mm}(t,t')$ depend on the correlation functions $\langle n_m(t) \rangle$ and $\langle d^+_m b c_{km} \rangle_t$ that have to be calculated self consistently. Notice that $\langle d^+_m b c_{km} \rangle_t$ is given by the following equation

$$
\langle d^+_m b c_{km} \rangle_{t + dt} = F_m(c_{km})/(2 * i)
$$
$$
= -(1/2) \left(\int_{t_0}^{t + dt} d\tau V_k(\tau) F_{mm}(\tau, t + dt) \right.
$$
$$
\times e^{i\epsilon_k(\tau - t - dt)} - (2n_{km} - 1) \int_{t_0}^{t + dt} d\tau V_k(\tau)
$$
$$
\left. \times G_{mm}(\tau, t + dt) e^{i\epsilon_k(\tau - t - dt)} \right)
$$

(21)

Then, an initial guess for $\langle d_m^+ bc_{km}\rangle_t$ is introduced in Eqs. (15) and (18) by using the following equation obtained by making the same approximations $[O(V^2)]$ leading to the equations of motion for the G and F:

$$id\langle d_m^+ bc_{km}\rangle_t/dt = (\epsilon_k - \varepsilon_m)\langle d_m^+ bc_{km}\rangle_t - z_m V_k n_{km} + V_k\langle n_m\rangle. \quad (22)$$

In this form $\langle d_m^+ bc_{km}\rangle$ is calculated at time $t+dt$ from the values determined at the preceding time t; and the atomic state occupation at the same time is obtained by using the exact equation

$$d\langle n_m(t)\rangle/dt = 2\,\mathrm{Im}\sum_k V_k(t)\langle d_m^+ bc_{km}\rangle_t. \quad (23)$$

Once the Green functions $F_{mm}(\tau,t+dt)$ and $G_{mm}(\tau,t+dt)$ with $t_0 < \tau \leq t+dt$ are calculated, the correlation function $\langle d_m^+ bc_{km}\rangle$ is obtained again at the time value $t+dt$ by using the integral expression (21) now, while $\langle n_m(t+dt)\rangle$ is recalculated from

$$\langle n_m(t+dt)\rangle = [G_{mm}(\tau \to t+dt, t+dt)$$
$$+ F_{mm}(t+dt, t+dt)]/(2i). \quad (24)$$

Notice that the approximate equation (22) does not yield the appropriate solution even for the case of a spinless Hamiltonian ($N=1$). Therefore it is only used for providing an initial guess, being then the correct value calculated by using the accurate expression (21) in terms of the time evolution of the G and F functions.

The interdependence of the occupation of a localized state with angular momentum projection m with the occupation of the other m' states, and also with the crossed terms $\langle d_{m'}^+ bc_{km'}\rangle$, is due to the strong intra-atomic correlation effects. In the particular case of $N=1$, our results [Eqs. (15) and (18)] recover the exact expressions for the spinless Hamiltonian, where only one active state is assumed in the atom site. The validity of this formalism for any value of N marks a difference with the NCA that is only well justified from a large-N expansion.[16]

III. RESULTS AND DISCUSSION

A. Semiclassical and static limit situations in the case of a N-fold degenerate d state

In this case $\varepsilon_m=\varepsilon_d$, $\langle n_m\rangle=n$, and $\Sigma\langle n_m\rangle=N*n=n_d$. The n_{km} are also independent of m, $n_{km}=n_k$.

1. Semiclassical limit

By using Eqs. (21) and (23) we have that

$$dn/dt = -\mathrm{Re}\left[\int_{t_0}^t d\tau \Xi^R(t,\tau)F_{mm}(\tau,t)\right.$$
$$\left. -\int_{t_0}^t d\tau \Omega(t,\tau)G_{mm}(\tau,t)\right]. \quad (25)$$

Notice that dn/dt in the infinite-U limit is determined only

by the crossed terms (Eq. (23)) as in the noncorrelated case, with the only difference of the boson operator that keeps memory of the infinite U-limit situation. This fact causes different time behaviors of the F and G functions in each case. The semiclassical approximation (SCA) to Eq. (25) is obtained by assuming $V_k(t)=Vu(t)$, and a constant density of states ρ for the metal. Then, the self-energies within this wide band-width approximation are

$$\Sigma^R(t,\tau) = -i\Theta(t-\tau)2\Delta(t)\delta(t-\tau),$$

$$\Omega(t,\tau) = -i2\Delta(t)\delta(t-\tau)$$
$$+ i2(\Delta_0/\pi)u(t)u(\tau)\int_{-\infty}^\infty d\epsilon \frac{\exp[-i\epsilon(t-\tau)]}{1+\exp[\beta(\epsilon-E_F)]},$$

where $\beta=1/k_B T$, $\Delta_0=\pi\rho V^2$, and $\Delta(t)=\Delta_0 u^2(t)$. By introducing these expressions for the self-energies in Eq. (25) and considering $F_{mm}(\tau,t)=f_{mm}(\tau,t)\exp[-i\varepsilon_d(\tau-t)]$, $G_{mm}(\tau,t)=g_{mm}(\tau,t)\exp[-i\varepsilon_d(\tau-t)]$, the following result is obtained:

$$dn/dt = \mathrm{Im}\left(-\Delta(t)[f_{mm}(t,t) + g_{mm}(t,t)]\right.$$
$$+ 2(\Delta_0/\pi)u(t)\int_{-\infty}^\infty \frac{d\epsilon}{1+\exp[\beta(\epsilon-E_F)]}$$
$$\left. \times \int_{t_0}^t d\tau u(\tau)\exp[-i(\epsilon-\varepsilon_d)(t-\tau)]g_{mm}(\tau,t)\right). \quad (26)$$

The SCA assumes that $g_{mm}(\tau,t)$ is a slowly varying function of τ and can be taken out of the integral in Eq. (26); this leads to[4]

$$dn/dt = \mathrm{Im}\{-\Delta(t)[f_{mm}(t,t) + g_{mm}(t,t)] + 2\Delta(t)f^<(\varepsilon_d)g_{mm}(t,t)\}$$

with $f^<(\varepsilon_d)=1/\{1+\exp[\beta(\varepsilon_d-E_F)]\}$. Finally, the SCA is only related with the state occupations

$$F_{mm}(t,t) + G_{mm}(t,t) = 2in,$$

$$G_{mm}(t,t) \to i\langle n_b(t) + n(t)\rangle.$$

The only difference introduced in the rate equation by the infinite U limit is the appropriate equal time behavior of the advanced physical Green function that also contemplates the $N=1$ case. The SCA result can be written as

$$dn/dt = 2\Delta(t)\{-n(t) + \langle n_b(t) + n(t)\rangle f^<(\varepsilon_d)\} \quad (27)$$

that is the same expression already obtained by Langreth et al.[4] within the NCA.

2. Static solution

The static limit is easily calculated assuming all the different self-energies to depend on $(t-\tau)$. This allows us to Fourier transform Eq. (15) to

$$G(\omega) = \frac{z_d - (N-1)I(\omega)}{\omega - \varepsilon_d - \Sigma_0(\omega) - (N-1)\Sigma_<}, \quad (28)$$
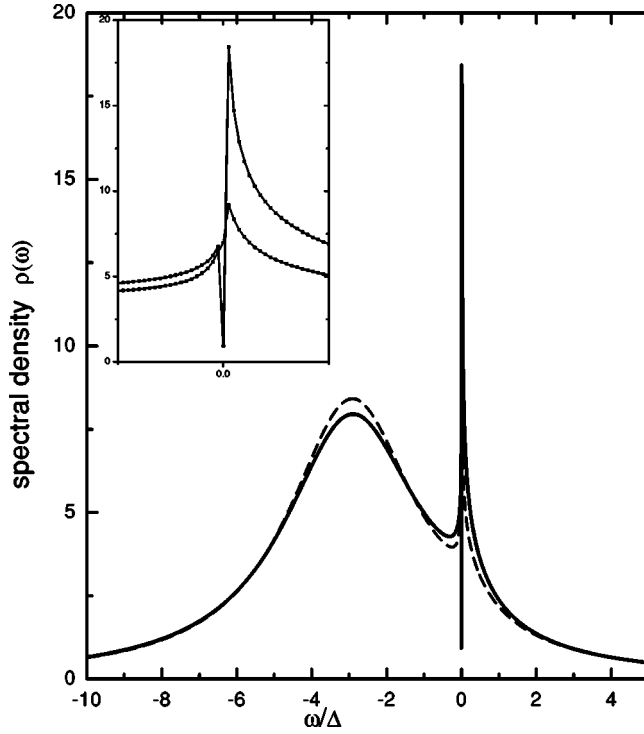
where:

FIG. 1. Spectral density for $N=2$ and $\epsilon_d=-0.04D$. The solid curve corresponds to the calculation derived from expression (34), and the dashed curve to the one from Lacroix approximation.

FIG. 2. The same as Fig. 1 for $\epsilon_d=0$. T_0 is the low energy scale deduced from the density of states.

$$\Sigma_0(\omega) = \sum_k \frac{V_k^2}{\omega - \epsilon_k - i\eta}, \qquad (29)$$

$$I(\omega) = \sum_k \frac{V_k \langle d^+ b c_k \rangle}{\omega - \epsilon_k - i\eta}, \qquad (30)$$

$$\Sigma_<(\omega) = \sum_k \frac{V_k^2 n_k}{\omega - \epsilon_k - i\eta}. \qquad (31)$$

The $\langle d^+ b c_k \rangle$ and $\langle n \rangle$ correlation functions are given by

$$\langle d^+ b c_k \rangle = (1/\pi) \int_{-D}^{D} d\omega' f_<(\omega') \mathrm{Im} \frac{V_k G(\omega')}{\omega' - \epsilon_k - i\eta}, \quad (32)$$

$$\langle n \rangle = \frac{1}{\pi} \int_{-D}^{D} d\omega' f_<(\omega') \mathrm{Im}\, G(\omega'), \qquad (33)$$

where D is the half-bandwidth and $f_<(\omega')$ is the Fermi distribution at temperature T.

Assuming V_k independent on k and $D \to \infty$, the spectral density of states $\rho(\omega) = \mathrm{Im}\, G(\omega)/\pi$ is found to be

$$\rho(\omega)$$

$$= \frac{\Delta_0/\pi}{[\omega - \varepsilon_d - (N-1)\mathrm{Re}\Sigma_<(\omega)]^2 + \Delta_0^2[1 + (N^2-1)f^<(\omega)]}.$$
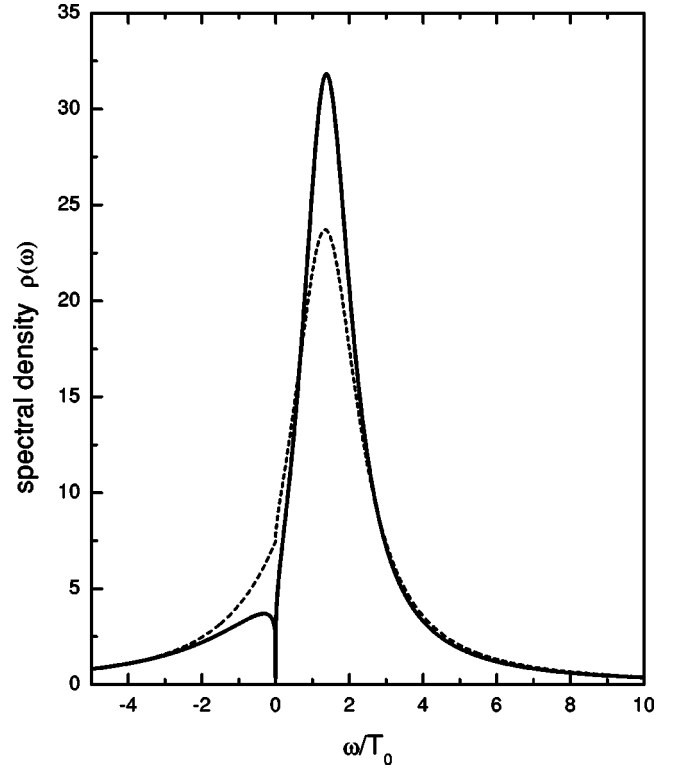$$(34)$$

The use of the decoupling terms given by Eqs. (11) and (12) leads to the proposal of Lacroix[14] for the spectral density of states, where also a self-consistent calculation with the correlation function $\langle c_K^+ c_k \rangle$ has to be performed.

Meir et al.,[12,13] by working within a pure fermionic description, neglected in the EOM the equal time boundary condition of Green functions such as $i\Theta(t'-t) \times \langle \{ d_\sigma^+(t'), d_{-\sigma}^+(t) c_{k-\sigma}(t) d_\sigma(t) \} \rangle$ that are the equivalent ones to the $G_m(d_{m'}^+ d_m c_{km'})$ in the slave-boson approach, see Eq. (9). Even though this might be a reasonable approximation at high temperatures, it is found that a poor description of the state occupations is obtained when neglecting the self-consistency with the crossed terms such as $\langle d_{-\sigma}^+(t) c_{k-\sigma}(t) \rangle$ at $T=0$ K.

Figures 1–3 show the spectral density $\rho(\omega)$ derived from Eq. (34) for $N=2$ and $T=0$ K, using $\Delta_0=0.01D$, and the following values for $\varepsilon_d=-0.04D$, 0.0, and 0.02D, respectively. In this form the three relevant regimes, Kondo, mixed-valence, and empty orbital, are covered. In the same figures we show the density of states obtained by using the Lacroix approximation.[14] Both solutions are very similar, except near the Fermi level where the Kondo resonance appears. While our approximation (34) yields zero density of states at the Fermi level and a too narrow Kondo peak, the Lacroix solution produces a finite value of the density of states at E_F—even though the Friedel-sum rule is far from being satisfied [$\rho(0) = \sin^2(\pi n_d/2)/\pi\Delta_0$]—and a very much diminished Kondo peak. When comparing with the NCA, we notice that the NCA presents a pathological cusp at the Fermi level. On the other hand, we found that the method presented
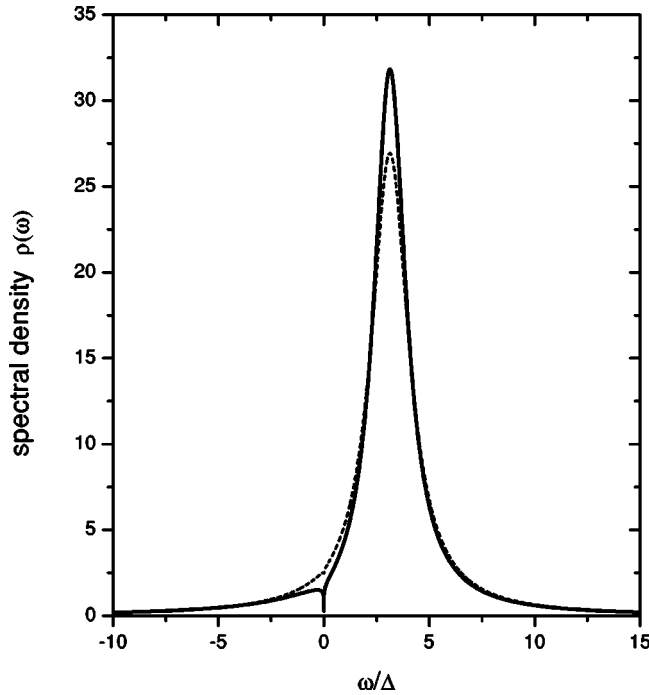
FIG. 3. The same as Fig. 1 for $\epsilon_d = 0.02D$.

in this work yields very accurate values for the atomic state occupation. The values for n_d by using Eq. (33) are 0.879, 0.306, and 0.182, which are very near to the exact ones obtained by using the NRG calculation 0.874, 0.314, and 0.172,[20] while the Lacroix approximation yields the following values: 0.88, 0.36, and 0.206. We will see below that this is also reflected in a better performance of our solution for dynamical cases.

Figures 4 and 5 show n_d as a function of $(\pi\varepsilon_d^*/N\Delta_0)$, where $\varepsilon_d^* = \varepsilon_d + [(N-1)\Delta_0/\pi]\ln(\pi D/N\Delta_0)$, for $N=2$ and $N=6$, respectively. The results of our approximation are compared with the ones from Lacroix approximation, with the exact results and those obtained from the leading order calculation of a $(1/N)$ expansion.[21] From these figures it is possible to appreciate the excellent occupation values that are obtained for a wide range of parameters when using the V^2 order calculation presented in this work.

B. Dynamical processes: Comparison with exact results

Our model system consists of a chain of four atoms, one representing the scattered particle and the other three the solid substrate, with a total number of electrons equal to 4. The three-atom substrate accounts for an incipient solid band formation and allows for an exact treatment of the dynamical charge exchange between the projectile and the discrete surface states. The exact solutions are obtained by solving the time-dependent Anderson Hamiltonian within the subspace of 36 many-electron configurations with a total spin component $S_z = 0$.[17,22] For the three-atom linear substrate the atom-atom hopping interaction is $\beta = -2$ eV, and the site energy is $\varepsilon_0 = 0.0$ eV. The energies of the band states are then $\epsilon_1 = -\sqrt{2}*|\beta|$, $\epsilon_2 = 0.0$, $\epsilon_3 = \sqrt{2}*|\beta|$. The time-dependent projectile-substrate hopping term is given by $V_k(t)$
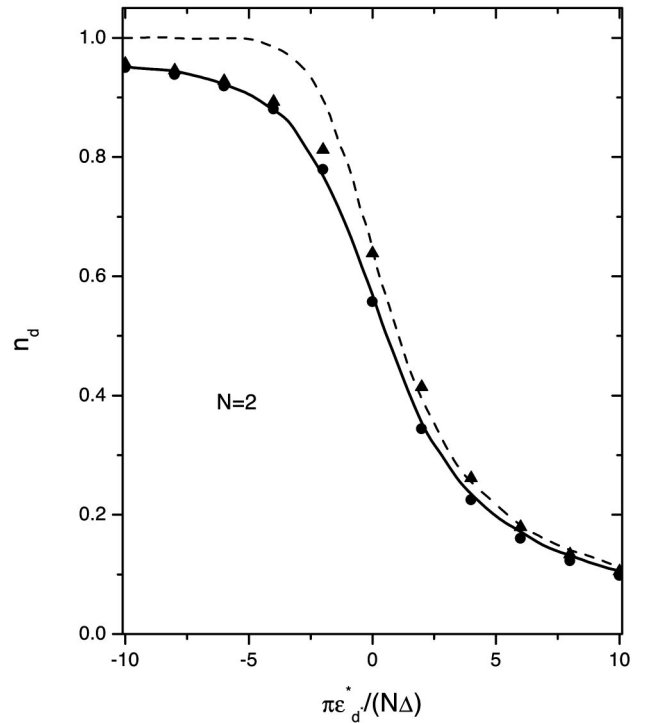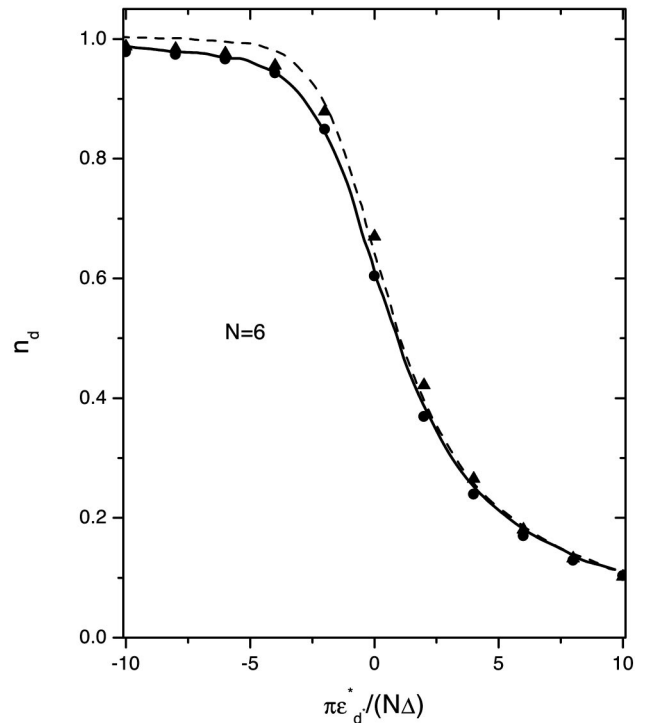

FIG. 4. The occupation n_d as a function of $\pi\varepsilon_d^*/N\Delta_0$, with ε_d^* defined in the text, for $N=2$. The full curve gives the exact results, and the dashed curve the leading order in a $1/N$ expansion (J. W. Rasul and A. C. Hewson, 1984). Full circles corresponds to the calculation of n_d derived from expression (33), and the full triangles to the one from Lacroix approximation.
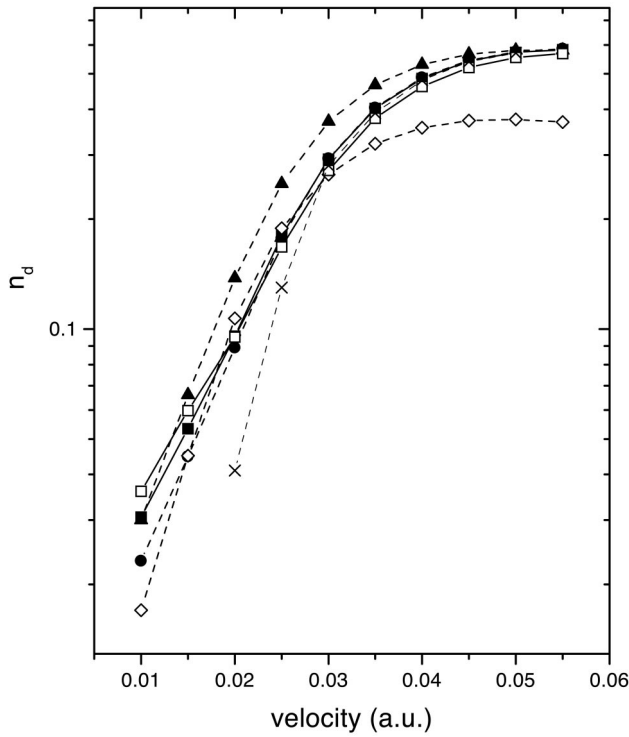

FIG. 5. The same as in Fig. 4, for $N=6$.

FIG. 6. The occupation n_d vs ion velocity for $\epsilon_d=-1$ eV. Empty and full squares correspond to the exact calculation using $U=10.0$ eV. and $U=50.0$ eV, respectively. Full circles correspond to our calculation (i) using Eqs. (15) and (18), full triangles to the calculation (ii) based on Lacroix approximation, and empty diamonds to the spin-less calculation (iii). The crosses correspond to the NCA results.

FIG. 7. The same as in Fig. 4 for $\epsilon_d=0$.

$=b_k V_0 \exp(-2v|t|)$, where v is the atom velocity, $V_0=-1.0$ eV, and b_k is the weight of the projectile first neighbor in the k-band state ($b_k=0.5$, $1./\sqrt{2}$, 0.5, for $k=1,2,3$ respectively). In the infinite-U limit approximation this model system corresponds to an N-fold degenerate state with $N=2$ (the spin-up and spin-down states). In all the cases we compare the exact results with (i) our approximation [Eqs. (15) and (18)], (ii) dynamical solution equivalent to Lacroix static approximation, (iii) a spinless solution where $N=1$ (this approach is often used to analyze the case of a very high electron-electron interaction). We also compare with the NCA results obtained by implementing Eqs. (20)–(23) of the work of Shao *et al.*.[5] for this four-level system.

Initially empty projectile spin states. In this case the four electrons occupy initially ($t=t_0$) the lowest energy band states ($\epsilon_k=\epsilon_1, \epsilon_2$), that means $n_k=1$ for $k=1,2$ and $n_k=0$ for $k=3$. The values of ϵ_d are chosen as representative of the different regimes in strong correlated systems interacting with a continuum band-state substrate: $\epsilon_d=-1.0$ eV (Kondo regime), $\epsilon_d=0.0$ eV (mixed-valence regime) and $\epsilon_d=1.0$ eV (empty-orbital regime). The U values used in the case of the exact calculation vary from 6.0 to 50.0 eV, depending on the atom velocity range. Figure 6 ($\epsilon_d=-1.0$ eV) and Fig. 8 ($\epsilon_d=1.0$ eV) show that for low velocities ($v \lesssim 0.02$ a.u.) the exact calculation reaches the infinite-U limit ($n_\uparrow=n_\downarrow$, $\langle n_\uparrow n_\downarrow \rangle$
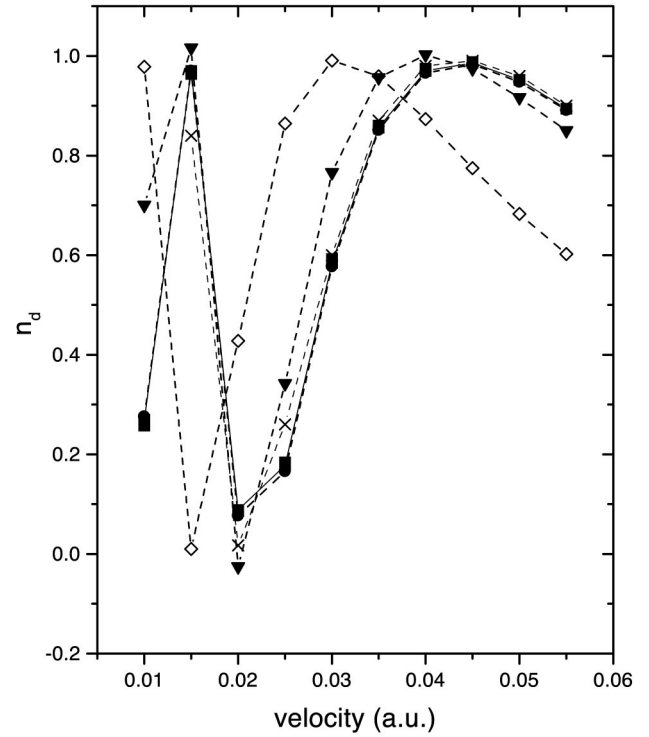
$\simeq 0$ and no dependence on U value) for values of U around 50.0 eV. While in the case of $\epsilon_d=0.0$ eV, Fig. 7, this limit is accomplished by $U \simeq 6.0$ eV in the whole velocity range. In this very discrete level system as the solid target, for $\epsilon_d=-1.0$ eV and $\epsilon_d=1.0$ eV a nearly adiabatic regime is being reached for $|v/\epsilon_d| \ll 1$ (in a.u.), and the requirement $U/V \gg 1$ becomes more restrictive to reproduce the infinite limit situation than in the well defined non adiabatic evolution. The probability of having one electron in the projectile site is given by $P_0=n_\uparrow+n_\downarrow=n_d$ in the infinite-U limit, while in the case of the spinless approximation this probability is given by the occupation n of the only one projectile state considered. In Figs. 6–8 the exact results of n_d as a function of the projectile velocity (in a velocity range from 0.01 a.u. to 0.055 a.u.) are compared with the results obtained by using the calculations i, ii, and iii and the NCA, for the three values of ϵ_d (-1.0 0.0, and 1.0 eV), respectively. From Figs. 6–8 it is concluded that in all the cases our calculation (i) is the best approximation to the exact results, not only with respect to the values of n_d, but also with respect to the velocity dependent behavior. The striking case is the $\epsilon_d=0.0$ eV one. The typical oscillatory behavior for a very discrete system within a resonant condition is obtained. Only the infinite-U limit approximation where the self-energies are calculated up to a V^2 order, is able to reproduce the marked oscillations of the exact results along the whole velocity range. When compared to the usual spinless approximation, the infinite-U limit calculation represents clearly an improvement, and it evidences the nonstraightforward predictable correlation effects in a dynamical process. Figures 6–8 also show the results obtained by using the NCA. We observe that for velocities $v \gtrsim 0.03$ a.u. the NCA reproduces the exact val-
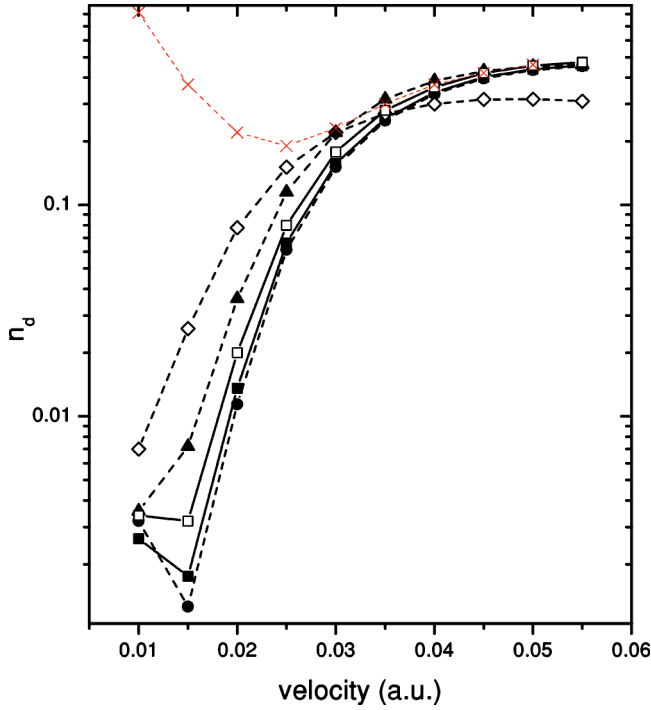
FIG. 8. The same as in Fig. 4 for $\epsilon_d = 1$ eV.

ues. In the low velocity range and for $\epsilon_d = -1.0$ eV (Fig. 6) this calculation underestimates the n_d values, but the most striking situation occurs for $\epsilon_d = 1.0$ eV (Fig. 8), where the NCA gives an unphysical growth of n_d for low velocities.

The average occupation for each spin-sate is shown as a function of time in Fig. 9, for the $\epsilon_d = 0.0$ eV case and a
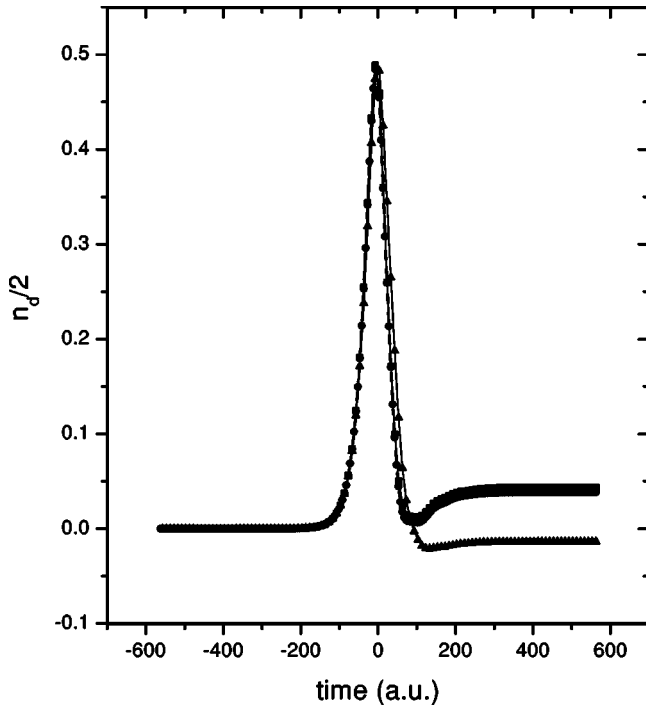

FIG. 9. Occupation per spin as a function of time for v $=0.02$ a.u. and $\epsilon_d = 0$. The same symbols as in Fig. 6 are used for the different calculations: i, ii, and exact.
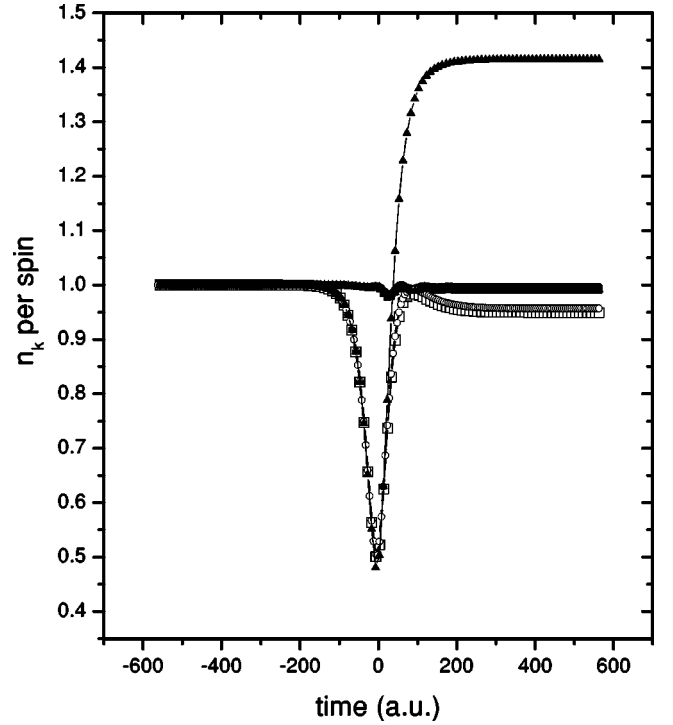

FIG. 10. Band-state occupations per spin as a function of time ($v = 0.02$ a.u., $\epsilon_d = 0.0$ eV). Square symbols correspond to the exact calculation, circles to our calculation (i) and triangles to the calculation (ii). Empty symbols correspond to $\langle n_{k\sigma} \rangle$ with $k=2$ and full ones to $\langle n_{k\sigma} \rangle$ with $k=1$ in the case of the exact and our calculation, while the opposite is valid for calculation (ii).

velocity value equal to 0.02 a.u. The results obtained by using (i) coincides practically with those from the exact calculation along the whole projectile trajectory, while the calculation (ii) gives a final average occupation slightly less than 0 in this case. In Fig. 10 the average occupations of the band states per spin $\langle n_{k\sigma}(t) \rangle$ are shown. These ones are calculated by using the exact relation

$$d\langle n_{k\sigma}(t)\rangle/dt = -2\,\text{Im}[V_k(t)\langle d^+_\sigma bc_{k\sigma}\rangle_t].$$

We find that the calculation (ii) yields $\langle n_{k\sigma}(t) \rangle > 1$ in some cases, reflecting a problem with the conservation of the number of total electrons $n_{\text{tot}} = n_d(t) + \Sigma_{km}\langle n_{km}(t) \rangle$, shown in Fig. 11; while our solution (i) presents a good behavior for the $\langle n_{k\sigma}(t) \rangle$, very close to the exact ones. This fact suggests strongly a lack of consistency when higher order terms with respect to the order V^2 criteria used to close the equation of motions are conserved in the self-energies.

We can also treat in a similar way the case in which the initial projectile charge configuration corresponds to a negative ion. In this case two electrons occupy the lowest energy band state ($\epsilon_k = \epsilon_1$), and the other two occupy the projectile state. The infinite-U limit calculation requires to think in term of holes, and in this form we have again that $\langle n_\uparrow n_\downarrow \rangle$ $\cong 0$. The calculation is performed by assuming initially the following hole-state occupations $n_k = 0$ for $k=1$, $n_k=1$, for $k=2,3$ and $n_\uparrow = n_\downarrow = 0$. The neutral charge state probability (P_0) is given by $n_d = n_\uparrow + n_\downarrow$ in the infinite-U limit, while in
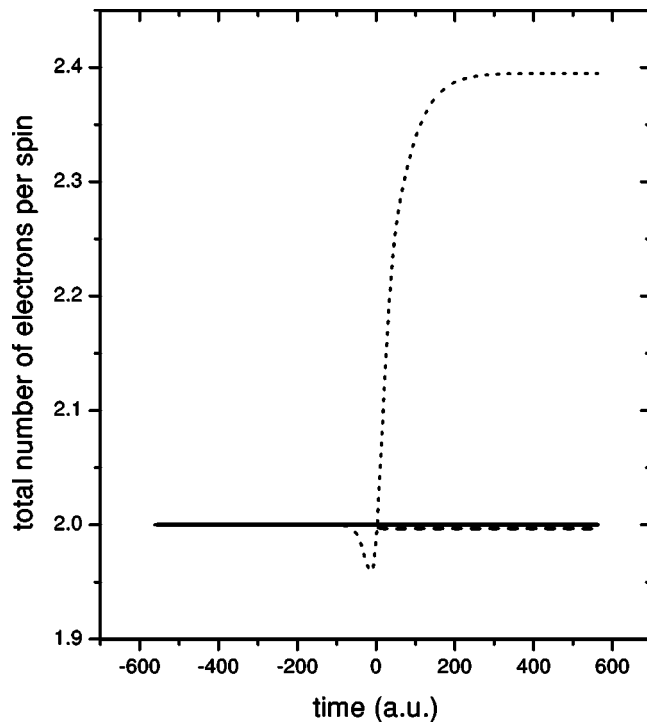
FIG. 11. Total number of electrons per spin as a function of time: $n_{tot}^\sigma = n_\sigma + \Sigma_k n_{k\sigma}$ ($v = 0.02$ a.u., $\epsilon_d = 0.0$ eV). Dashed line corresponds to our calculation (i), and the dot line to the calculation (ii). Solid line corresponds to the exact calculation.

the spinless calculation $P_0 = n$, where n is in this case the occupation of the only one hole-state considered. The energy ϵ_d corresponds now to the energy level for the second electron, that is $\epsilon_d = \epsilon_d^* + U$, where ϵ_d^* and U are, respectively, the atom energy level and the Coulomb repulsion parameter used

in the exact calculation. Due to the symmetries of the problem, the same neutral charge probabilities are obtained for the incoming negative ion with $\epsilon_d = -1.0$ eV and the incoming positive ion with $\epsilon_d = 1.0$ eV (Fig. 8); the incoming negative ion with $\epsilon_d = 1.0$ eV and the incoming positive ion with $\epsilon_d = -1.0$ eV (Fig. 6); and finally the incoming negative ion and the incoming positive ion with $\epsilon_d = 0.0$ eV (Fig. 7).

IV. CONCLUSIONS

A solution for the infinite-U limit is found by using the physical Green functions of the slave-boson approach to the Anderson Hamiltonian and solving the equations of motion up to a V^2 order. We obtain in this form accurate results for static and dynamical situations shown by the comparison with exact calculations. The integro-differential equations for the Green functions are solved in a consistent way with the correlation functions related with the atom state occupation and the atom-surface crossed terms, thus leading to the very accurate results obtained. While we find a lack of consistency when higher order terms are not introduced appropriately. Our calculation allows to treat a N-fold of localized states on the atom site for any value of N, reproducing the exact result for the $N=1$ case.

[1] A. C. Hewson, *The Kondo Problem to Heavy Fermions* (Cambridge University Press, Cambridge, 1993).

[2] P. Fulde, *Electron Correlations in Molecules, Atoms, and Solids* (Springer, Berlin, 1995).

[3] D. Goldhaber-Gordon, Hadas Shtrikman, D. Mahalu, D. Abusch-Magder, U. Meirav, and M. A. Kastner, Nature (London) **391**, 156 (1998).

[4] D. C. Langreth and P. Nordlander, Phys. Rev. B **43**, 2541 (1991).

[5] H. Shao, D. C. Langreth, and P. Nordlander, Phys. Rev. B **49**, 13 929 (1994).

[6] H. Shao, P. Nordlander, and D. C. Langreth, Phys. Rev. B **52**, 2988 (1995).

[7] H. Shao, P. Nordlander, and D. C. Langreth, Phys. Rev. Lett. **77**, 948 (1996).

[8] J. Merino and J. B. Marston, Phys. Rev. B **58**, 6982 (1998).

[9] P. W. Anderson, Phys. Rev. **124**, 41 (1961).

[10] P. Coleman, Phys. Rev. B **29**, 3035 (1984).

[11] L. V. Keldysh, Zh. Eksp. Teor. Fiz. **47**, 1515 (1964) [Sov. Phys. JETP **20**, 1018 (1965)].

[12] Y. Meir, N. S. Wingreen, and P. A. Lee, Phys. Rev. Lett. **66**, 3048 (1991).

[13] Y. Meir, N. S. Wingreen, and P. A. Lee, Phys. Rev. Lett. **70**, 2601 (1993).

[14] C. Lacroix, J. Phys. F: Met. Phys. **11**, 2389 (1981).

[15] N. Sergueev, Qing-feng Sun, Hong Guo, B. G. Wang, and Jian Wang, Phys. Rev. B **65**, 165303 (2002).

[16] N. E. Bickers, Rev. Mod. Phys. **59**, 845 (1987).

[17] T. L. Einstein, Phys. Rev. B **11**, 577 (1975).

[18] E. C. Goldberg and M. C. G. Passeggi, J. Phys.: Condens. Matter **8**, 7637 (1996).

[19] E. C. Goldberg, P. G. Bolcatto, R. Monreal, and F. Flores, Nucl. Instrum. Methods Phys. Res. B **182**, 49 (2001).

[20] T. A. Costi, J. Kroha, and P. Wolfle, Phys. Rev. B **53**, 1850 (1996).

[21] J. W. Rasul and A. C. Hewson, J. Phys. C **17**, 2555 (1984).

[22] E. C. Goldberg, E. R. Gagliano, and M. C. G. Passeggi, Phys. Rev. B **32**, 4375 (1985).